J Mater Sci: Mater Electron (2016) 27:913–920
DOI 10.1007/s10854-015-3834-1

Effect of B-site dopants Nb, Ta and W on microstructure and electrical properties of $Ca_{0.85}(Li, Ce)_{0.075}Bi_4Ti_4O_{15}$-$0.01MnCO_3$ piezoelectric ceramics

Deqiong Xin[1] · Zhihang Peng[1] · Fengkang Huang[1] · Qiang Chen[1] · Jiagang Wu[1] · Yadan Wang[1] · Xi Yue[1] · Dingquan Xiao[1] · Jianguo Zhu[1]

Received: 17 June 2015 / Accepted: 5 October 2015 / Published online: 17 October 2015

Abstract (Li, Ce) and Mn modified $CaBi_4Ti_4O_{15}$ (CBT) based ceramics were prepared by the solid state route, and were substituted by the equimolar ions of Nb^{5+}, Ta^{5+} and W^{6+} in the B-site. The variations of crystalline structure, microstructure, piezoelectric properties and dielectric properties were investigated. The XRD patterns indicated that all compositions formed a single bismuth layered-structural phase with $m = 4$. The additions of Nb_2O_5, Ta_2O_5 and WO_3 into CBT-based ceramics were found to affect the electrical properties and temperature stability of the ceramics. Compared with Ta_2O_5 and WO_3, the Nb-substitued ceramics exhibited the optimum piezoelectric property and dielectric property ($d_{33} \sim 19.6$ pC/N, $\varepsilon_r \sim 123.7$ and $\tan\delta \sim 0.1$ %) among all of these samples, together with a high Curie-temperature ($T_C \sim 767.6$ °C). Thermally activated depolarization behavior also demonstrated that the Nb^{5+} doped CBT-based ceramics possess outstanding thermal stability of piezoelectric properties. These results indicated that Nb_2O_5 has a substantial effect on the structure and properties of CBT-based ceramics compared to Ta_2O_5 and WO_3.

1 Introduction

Lead-based $Pb(Zr,Ti)O_3$ piezoelectric ceramics (PZT) possess outstanding performance and have been widely used in various fields [1, 2]. However, owing to the large content of toxic raw materials PbO or Pb_3O_4, PZT ceramics potentially trigger some environmental concerns during the manufacture and utilization processes [3]. Furthermore, the relatively low Curie-temperature ($T_C < 380$ °C) hinders their application in some hazardous environment. Nowadays, sensors in some industries referring to gas turbine, aero-engine and nuclear power have expressed strong demands for a good sensitivity over a broad temperature range. Bismuth layered-structured ferroelectrics (BLSFs) have a general formula of $(Bi_2O_2)^{2+}$ $(A_{m-1}B_mO_{3m+1})^{2-}$, whose structure is that pseudo-perovskite layers $(A_{m-1}B_mO_{3m+1})^{2-}$ and $(Bi_2O_2)^{2+}$ layers alternatively stack in the c-axis direction. A in the formula is a cation with a coordination number of 12. Its candidates include cations from monovalent to tetravalent or their combination, such as K^+, Na^+, Sr^{2+}, Ca^{2+}, Ba^{2+}, Pb^{2+}, Bi^{3+}, La^{3+}, Y^{3+}, Th^{4+} and U^{4+}. B is a transition metal cation with a coordination number of 6, such as Fe^{3+}, Ga^{3+}, Cr^{3+}, Zr^{4+}, Ti^{4+}, Nb^{5+}, Ta^{5+}, W^{6+} and Mo^{6+}, and m represents the number of the perovskite layers sandwiched between the bismuth oxide layers [4–19]. BLSFs, who possess a high Curie-temperature T_C, are promising candidates for high temperature applications. However, their practical usage in high temperature sensors is limited by the relatively low piezoelectric coefficient. In order to improve the piezoelectric properties, A and B site substitutions are widely used [9–19].

It has been reported that the chemical modification is an effective way to improve the piezoelectric properties of BLSFs in recent years. Among numerous BLSFs, $CaBi_4Ti_4O_{15}$ (CBT) ceramic is a typical four-layered BLSFs which possesses high $T_C = 790$ °C [20]. But it has some obvious shortcomings, such as low electromechanical coupling factor ($k_t < 10$ %), large temperature coefficient of resonance frequency ($fr \cdot T_C = 4 \times 10^{-5}$/ °C) and low d_{33} value (~ 5 pC/N) [17]. Therefore, much work has focused

✉ Jianguo Zhu
nic0400@scu.edu.cn

[1] College of Materials Science and Engineering, Sichuan University, Chengdu 610064, People's Republic of China

on the doping of A-site or B-site to enhance the piezoelectric property of CBT-based ceramics.

It was reported that moderate (Li, Ce) doped CBT-based ceramics increased T_C up to 866 °C and significantly improved d_{33} value to about three times of that in pure CBT ceramics (~20 pC/N) [21]. The dopants (Li, Ce) in the A-site of pseudo-perovskite unit can effectively enhance the chemical stability of oxygen vacancies by improving the height of the potential barrier for hopping. In addition, A-site dopants can change the domain structures that result in enhancement of the mobility of the domain [22, 23].

B-site is transition metal cations, they have similar ionic radii. So they do not make a major contribution to structural distortion which is responsible for the polarization of BLSFs [21]. However, owing to the volatilization of bismuth element during the sintering process, the conduction mechanism of BLSFs usually exhibits *p*-type conduction in nature. Higher valence cations, such as Nb^{5+}, Ta^{5+} and W^{6+}, were introduced as donor dopants. They could compensate the oxygen vacancies that results in enhancement of the remnant polarization and the resistivity. This method could improve the piezoelectric properties [22–24]. Jiangtao Zeng et al. [25] studied the W-doped CBT ceramics. The d_{33} value increases to 10 pC/N when W^{6+} doping content is 0.025 mol%. Furthermore, it has been reported that the dielectric property and piezoelectric property are improved in $MnCO_3$-doped CBT ceramics. In addition, the density and resistivity of the ceramics are also improved [26, 27]. As is known to all, these studies and reports mainly focus on the effect of the doping amount on the structure, ferroelectric, dielectric and piezoelectric properties of CBT. However, there is less comparative investigations for the effect of Nb^{5+}, Ta^{5+} and W^{6+} ion doping on the microstructure and properties, especially the equivalence in dopants amount and variation in doping types.

In this paper, various B-site dopants Nb, Ta and W, were introduced to (Li, Ce) and Mn modified CBT ceramics. $Ca_{0.85}(Li, Ce)_{0.075}Bi_4Ti_{3.98}M_{0.02}O_{15}-0.01MnCO_3$ (M = Nb, Ta, W) ceramics were prepared, and the comparative study of the lattice microstructure and electrical properties was performed.

2 Experimental procedure

$Ca_{0.85}(Li, Ce)_{0.075}Bi_4Ti_{3.98}M_{0.02}O_{15}-0.01MnCO_3$ (abbreviated as CBT-Nb, CBT-Ta, and CBT-W, M = Nb, Ta, W) ceramics were prepared by the conventional solid-state reaction method. The starting raw materials were Bi_2O_3(99 %), $CaCO_3$ (99 %), TiO_2(98 %), Li_2CO_3(99.99 %), CeO_2(99.99 %), $MnCO_3$(98.4 %), Nb_2O_5(99.99 %), Ta_2O_5(99.99 %) and WO_3(99 %). All powders were weighed according to the stoichiometric proportion and ball milled in the nylon jars with ethanol as a media for 24 h. Mixtures were dried and then calcined at 800 °C for 2 h. After calcination, mixtures were milled again in the same condition. The powders were dried and granulated with polyvinyl alcohol (PVA) as a binder. The powders were pressed into disks of 10 mm in diameter and 0.9 mm in thickness. After burning out the PVA at 700 °C, the green plates were finally sintered at 1080–1120 °C for 2 h according to the composition.

The densities of ceramics were measured by the Archimedes method. The crystal structure of samples were determined by X-ray diffractometer (DX2700, Dandong, China) and Rietveld refinement method. Before the measurements of electrical properties, the ceramics were pasted silver electrodes and fired at 700 °C for 10 min. The piezoelectric coefficient d_{33} value was obtained by a quasi-static d_{33} meter (ZJ-3A, Institute of Acoustics, Academia Sinca, China). The frequency dependence of dielectric properties for samples was measured by a precision impedance analyzer (HP4294A, Agilent, US). Temperature dependence of the dielectric properties were determined using an LCR analyzer (HP 4980A, Agilent, US) in temperature range of 30–830 °C.

3 Results and discussion

Figure 1 shows the XRD patterns of the B-site substituted CBT ceramics. The diffraction peaks were indexed referring to the PDF card# 52-1640, showing that all compositions belong to the typical Aurivillius type phase structure with $m = 4$. The highest intensity of diffraction peak is correlated to the (119) orientation, which is consistent with the fact that the most intense diffraction peak of the BLSFs is the type of (112 $m \pm \underline{1}$) [28]. No secondary phase is found in all the samples, which indicates that B-site

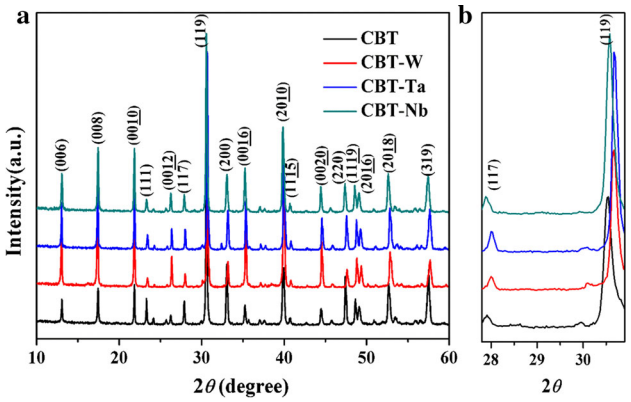

Fig. 1 The XRD patterns for CBT and CBT-M (M = Nb, Ta, W) ceramics

dopants Nb, Ta and W have fully diffused into the CBT lattice and formed the solid solutions. It is noted that the diffraction peaks shift to lower angles, when the B-site Ti^{4+} of CBT is substituted by W^{6+}, Ta^{5+} to Nb^{5+}, respectively. This variation indicates that the lattice parameters increase, which is attributed to the radius of substitution are gradually increased ($r_{Ti}^{4+} \sim 0.605$ Å, $r_{Nb}^{5+} \sim 0.69$ Å, $r_{Ta}^{5+} \sim 0.64$ Å and $r_{W}^{6+} \sim 0.60$ Å).

To further analyze the structural features of CBT-M (M = Nb, Ta, W) ceramics, XRD patterns were performed Rietveld refinement [29] using the Maud software [30]. The observed and calculated data from XRD patterns of CBT-M (M = Nb, Ta, W) ceramics are shown in Fig. 2. The bottom of the figures show their differences. The best fitting between observed and calculated intensities were obtained with space group A21am in the Orthogonal Symmetry. The detailed structure parameters and atomic positions are shown in Table 1. As the B-site dopant changes, the atomic positions of Ca, Bi, Ti and O also change with the same space group and Symmetry. It indicates that the different dopants Nb, Ta and W in B-site cause the different lattice distortion.

Except for the atomic positions movement, Fig. 3 shows the lattice parameter *a*, *b* and *c* values calculated by Rietveld refinement method. It can be found that the lattice parameters *a*, *b* and *c* values of CBT-M are all bigger than pure CBT. The lattice parameter *b* and *c* value increases, whereas *a* value decreases gradually with increasing radii of B-site dopants W, Ta and Nb. The variations of *a* and *b* originate from the distortion of BO_6 octahedra [31]. In addition, it is well known that the tolerance factor *t* is introduced to depict the lattice distortion of perovskite structure compounds [32]. The tolerance factor for perovskite structure is given by $t = (r_A + r_O)/\sqrt{2}(r_B + r_O)$, where r_A, r_B and r_O are respectively the ionic radii of A-site cation, B-site cation and oxygen ion [32, 33]. The ionic radii of W^{6+}, Ta^{5+} and Nb^{5+} are 0.60, 0.64 and 0.69 Å, respectively. Hence, the increasing of doping ionic radii leads to the decreasing of *t* value, and also results in the increasing of structural distortion. Thus, CBT-Nb ceramic possesses the most obvious lattice distortion.

Figure 4 a/a′, b/b′ and c/c′ show the SEM images magnified 2 k/8 k times for the natural surface of the CBT-Nb, CBT-Ta and CBT-W ceramics. Three samples all show the

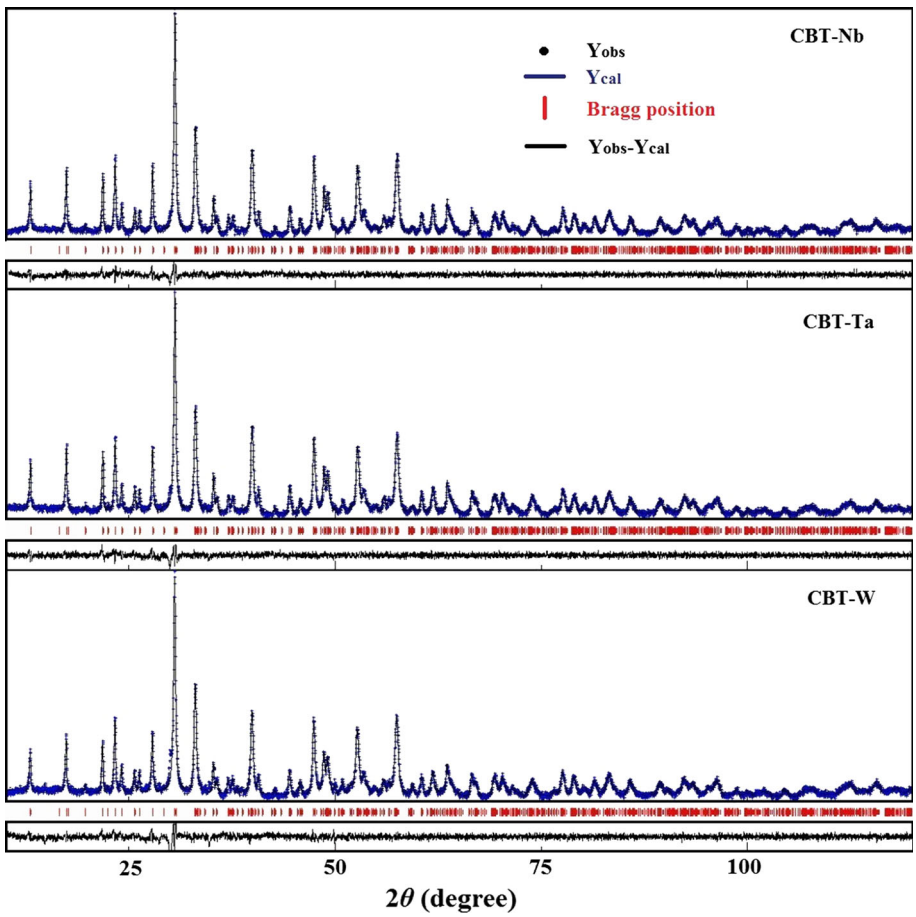

Fig. 2 Rietveld refinement on XRD patterns of CBT and CBT-M (M = Nb, Ta, W) ceramics

Table 1 Crystal structure parameters of CBT and CBT-M (M = Nb, Ta, W) ceramics are derived from the Rietveld refinement program

Parameters		CBT (model)	CBT-Nb	CBT-Ta	CB-W
Rw (%)		–	10.90	10.63	12.71
Rb (%)		–	7.99	7.83	9.09
Sig.		–	1.28	1.26	1.45
Symmetry		Orthogonal	Orthogonal	Orthogonal	Orthogonal
Space group		$A2_{1am}$	$A2_{1am}$	$A2_{1am}$	$A2_{1am}$
a(Å)		5.4234	5.4311	5.4310	5.4254
b(Å)		5.4021	5.4142	5.4144	5.4219
c(Å)		40.5935	40.7507	40.7537	40.7629
Atomic position	Occupancy				
Bi1	1	0.25, 0.2698, 0.2190	0.2505, 0.2703, 0.2189	0.2574, 0.2726, 0.2189	0.2642, 0.2724, 0.2190
Bi2	0.6	0.2464, 0.2520, 0	0.2583, 0.2392, 0	0.2578, 0.2418, 0	0.2482, 0.2440, 0
Bi3	0.7	0.2452, 0.2438, 0.8956	0.2414, 0.2421, 0.8957	0.2487, 0.2436, 0.8956	0.2493, 0.2422, 0.8952
Ca1	0.4	0.2464, 0.2520, 0	0.2583, 0.2392, 0	0.2578, 0.2418, 0	0.2482, 0.2440, 0
Ca3	0.3	0.2452, 0.2438, 0.8956	0.2414, 0.2421, 0.8957	0.2487, 0.2436, 0.8956	0.2493, 0.2422, 0.8952
Ti1	1	0.2148, 0.2478, 0.5492	0.2095, 0.2356, 0.5492	0.2236, 0.2382, 0.5493	0.2102, 0.2473, 0.5493
Ti2	1	0.2155, 0.247, 0.3482	0.2157, 0.2504, 0.3459	0.2166, 0.2422, 0.3465	0.2162, 0.2564, 0.3460
O1	1	0.679, 0.3250, 0	0.8848, 0.1257, 0	0.8329, 0.0955, 0	0.8709, 0.1396, 0
O2	1	0.4735, 0.4678, 0.5402	0.4375, 0.5069, 0.5447	0.5758, 0.4979, 0.5439	0.5110, 0.4631, 0.5446
O3	1	0.4014, −0.047, 0.5523	0.4520, 0.0658, 0.5370	0.4617, 0.0494, 0.5391	0.4282, −0.0095, 0.5388
O4	1	0.986, 0.496, 0.2502	1.0228, 0.4868, 0.2562	1.0675, 0.4929, 0.2570	1.0697, 0.5065, 0.2575
O5	1	0.1915, 0.3106, 0.4048	0.3207, 0.3338, 0.4074	0.3248, 0.3458, 0.4077	0.3290, 0.3359, 0.4081
O6	1	0.4304, 0.5282, 0.3528	0.4814, 0.4193, 0.3555	0.4702, 0.4350, 0.3548	0.4418, 0.4778, 0.3570
O7	1	0.4683, 0.0142, 0.3612	0.4489, 0.0274, 0.3643	0.4919, 0.0416, 0.3653	0.4936, 0.0498, 0.3650
O8	1	0.215, 0.1976, 0.6951	0.3048, 0.1765, 0.6971	0.3299, 0.1943, 0.6970	0.3464, 0.2088, 0.6892

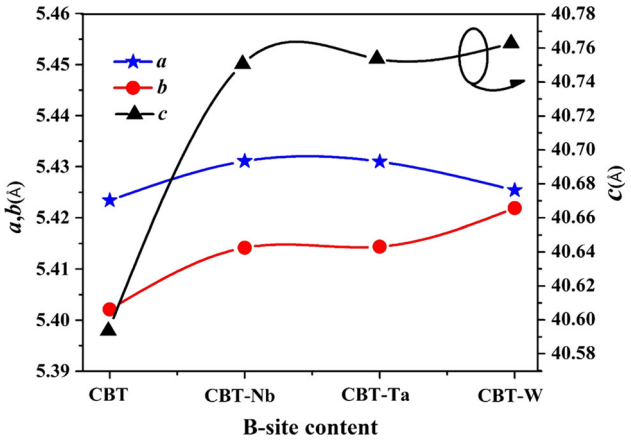

Fig. 3 The lattice parameters *a*, *b*, *c* for CBT and CBT-M (M = Nb, Ta, W) ceramics

disc shaped grains which is attributed to the highly anisotropic grain growth rate in the direction of the *a*–*b* plane and along the *c*-axis. This anisotropic microstructure is the typical feature of Aurivillius type compounds [29, 34, 35]. It can be seen that CBT-Nb and CBT-Ta ceramics present well-packed and pore-free microstructures indicating their high density. However, the grain size of CBT ceramics decreases with the introduction of W^{6+} dopants. The average grain size values with error bars of CBT-M are shown in Fig. 3d. The grain size of CBT-Nb and CBT-Ta ceramics in length scale is found to be ~7 μm, but decreases to ~5 μm in W^{6+} doping specimen. Nevertheless, the grain size in the thickness of all specimens is ~0.6 μm. Hence, the ratio of length and thickness significantly decreases with W^{6+} additives, implying that WO_3 delays the diffusion mechanisms and decreases the anisotropic feature of microstructure. Furthermore, more homogeneous grain is found in CBT-Nb specimen that possesses the highest density among the specimens.

Figure 5 shows the d_{33} values and relative density of three samples CBT-Nb, CBT-Ta, CBT-W at room temperature. It can be obviously found that with the B-site doping varying from Nb^{5+} to W^{6+} in CBT ceramics, the relative density gradually decreases. Nb^{5+}-modified CBT ceramics possess the largest relative density (~96.6 %). The effect of the high valence substitution in B-sites on the densification of CBT ceramics was primarily due to two factors. One factor is the crystal distortion of the oxygen octahedral caused by the difference in size and valence between substituted-ions and Ti^{4+}. The distortion induced the enhancement of the density in CBT ceramics to some extent [36]. The other factor is the low melting point of the substitution. Compared to Ta_2O_5 and WO_3, the melting point of Nb_2O_5 is the lowest. Introducing Nb_2O_5 into the CBT ceramics reduces the energy battier for the diffusion of particles, which is helpful to the grain growth during the sintering process and form the densification CBT ceramics. The SEM image of pure CBT ceramic shows the formation of plate-like grains with different sizes which are inhomogeneously distributed, and the relative density is only 94 % [20], which is lower than that of the CBT-Nb ceramics.

It can be seen in the Fig. 5, the piezoelectric constant d_{33} value gradually decreases. The CBT-Nb ceramics possess

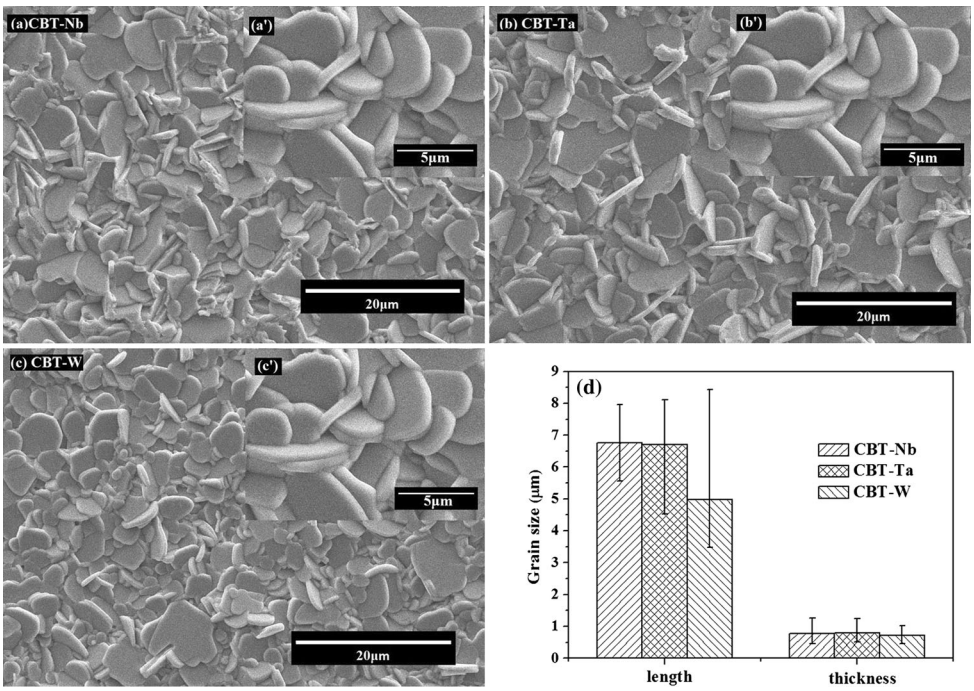

Fig. 4 **a**–**c** The 2 k times magnified SEM images for CBT-M (M = Nb, Ta, W) ceramics. a′–c′ The 8 k times magnified SEM images for CBT-M (M = Nb, Ta, W) ceramics. **d** The grain sizes for CBT-M (M = Nb, Ta, W) ceramics

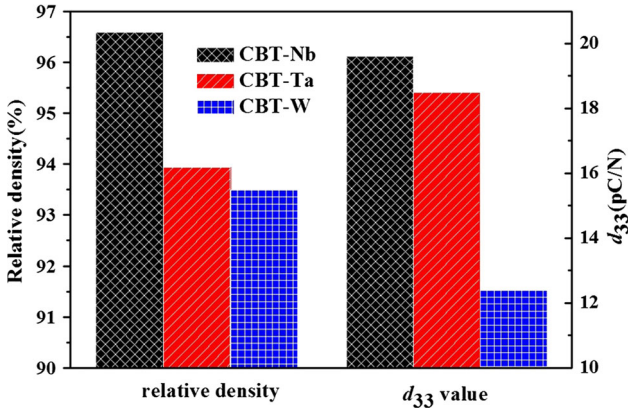

Fig. 5 The relative density and d_{33} values for CBT-M (M = Nb, Ta, W) ceramics

the optimum d_{33} value (19.6 pC/N), which is much higher than that of (Li, Ce) co-doped $CaBi_4Ti_4O_{15}$ ceramics (~15 pC/N) [17]. Furthermore, the d_{33} values of CBT-Ta and CBT-W ceramics are 18.5 pC/N and 12.4 pC/N, respectively, they both exceed that of 0.025 mol% W doped $CaBi_4TI_4O_{15}$ ceramics (~10 pC/N) [25]. The increase in density of CBT is benefit for the piezoelectric properties. In addition, it is reported that the domain motion is much easier in larger grains than that in smaller sized grains, that is to say, the increase in grain size improves the piezoelectric properties [37]. It can be seen in Fig. 4d, the substitution of Nb increases the average grain size, it is reasonable to enhance the d_{33} value of CBT ceramics to a higher level as compared to Ta and W doped CBT ceramics.

Figure 6 shows the thermal depolarization behavior of CBT-based ceramics. The d_{33} value of three samples gradually decreases with rising annealing temperature. This degradation is attributed to the reverse switching of non-180° ferroelastic domains stimulated by the thermal and/or mechanical activation [38]. The d_{33} value drops to zero when the annealing temperature is above the T_C, indicating an involvement of ferro-paraelectric phase transition. According to the report of Chen et al. [17], effect of thermal depoling on the piezoelectric properties for (Li, Ce) co-doped CBT ceramics are more obvious. When the annealing temperature increases to 600 °C, d_{33} value which reduces from 15 to 11 pC/N, only remains 73 % of the original value. However, in this experiment, d_{33} value of CBT-Nb retains 16.4 pC/N after annealing at 600 °C, which remains 84 % of the initial value. This suggests that the CBT-Nb ceramics possess good thermal stability of piezoelectric properties.

Figure 7 shows the frequency dependence of dielectric permittivity (ε_r) and loss (tanδ) for the CBT-based ceramics at room temperature. As can be seen in Fig. 6, the permittivity for CBT-M is higher than that of pure CBT ceramics, but the dielectric loss is lower than that of pure CBT. Moreover, the dielectric loss of each sample rapidly decreases in the frequency range of 10^3–10^4Hz. The polarization of defect dipoles is mainly responsible for the dielectric loss in this frequency range. Nevertheless, with further increasing frequency, ε_r and tanδ decrease slightly, which demonstrates excellent stability of dielectric properties for CBT-based ceramics in high-frequency.

Figure 8 shows the temperature dependence of the permittivity (ε_r) and loss (tanδ) for the poled CBT-based ceramics at the frequency of 1 MHz. The permittivity increases with the increasing temperature and the maximum value appears at T_C which is corresponding to the ferro-paraelectric phase transition. The CBT-Nb ceramics possess the highest T_C value of 767.6 °C, three samples own nearly the same T_C value, within the error range. And they approximate the T_C of pure CBT (790 °C). The Curie temperature (T_C) is strongly associated with the ionic radii of A-site cations. The radii of A-site dopants (Li, Ce) (1.25 Å) is smaller than Ca^{2+} (1.34 Å) [21]. It causes more

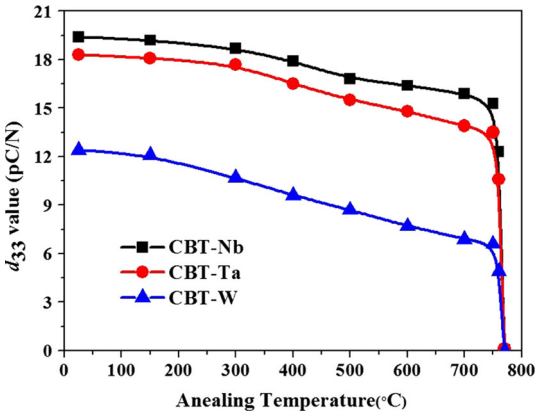

Fig. 6 The thermal depoling behavior of CBT-M (M = Nb, Ta, W) ceramics

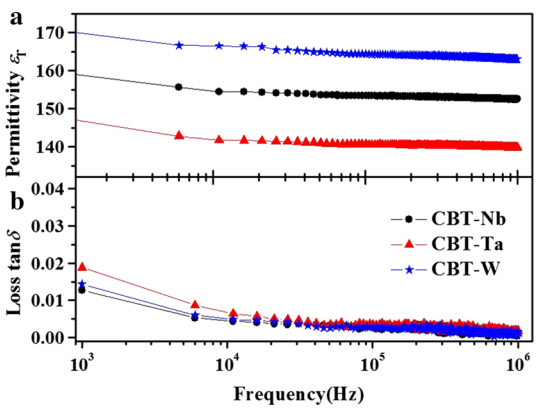

Fig. 7 Frequency dependence of **a** permittivity (ε_r) and **b** loss (tanδ) for CBT-M (M = Nb, Ta, W) ceramics

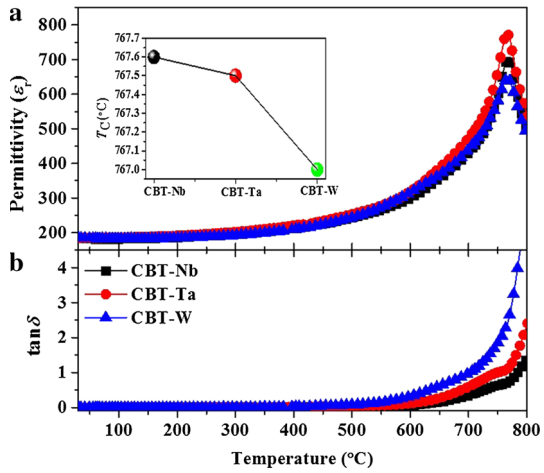

Fig. 8 Temperature dependence of **a** permittivity (ε_r) and **b** loss (tanδ) for CBT-M (M = Nb, Ta, W) ceramics

obvious structural distortion, which leads to a higher T_C value [39, 40]. It was reported that the dielectric loss of $Ca_{0.85}(Li, Ce)_{0.075}Bi_4Ti_4O_{15}$ ceramics was up to 0.579 % [9], and the dielectric loss of $CaBi4Ti_{4-x}W_xO_{15}$ ($x = 0.025$) ceramics increased fast above 400 °C [25]. It is found that the dielectric loss of CBT-Nb ceramics remains low value ($\sim$0.15 %) below 600 °C. However, with further increasing temperature, the loss value gradually increases, especially at the temperature above 700 °C, owing to the decrease of electrical resistivity. Furthermore, it is noted that the CBT-Nb ceramics possess the lowest loss value among all compositions, indicating that Nb substitution obviously improves temperature dependence of dielectric properties.

4 Conclusions

In summary, $Ca_{0.85}(Li, Ce)_{0.075}Bi_4Ti_{3.98}M_{0.02}O_{15}-0.01MnCO_3$ (M = Nb, Ta, W) ceramics were prepared by conventional solid-state reaction method. XRD patterns indicate that B-site modified CBT-based ceramics own the typical Aurivillius type phase structure. After comparing the structures and electrical properties of three compositions, the CBT ceramics doped by Nb^{5+} in B-site show the optimum properties. The relative density and the piezoelectric coefficient d_{33} value are 96.6 % and 19.6 pC/N, respectively. In addition, the piezoelectric property of the CBT-Nb ceramic possesses a good temperature stability which can be well proved via its thermal depoling behavior. The T_C(767.6 °C) of Nb^{5+} doped CBT ceramics is higher than that of Ta^{5+} and W^{6+} doped CBT. The frequency dependence of the dielectric permittivity (ε_r) and loss (tanδ) demonstrate the frequency stability of CBT-Nb ceramics. As a result, the addition of Nb plays a significant role in the microstructure and electric properties of CBT-based ceramics, which shows a potential for high-temperature sensor applications.

Acknowledgments This work was supported by the National Natural Science Foundation of China (NSFC Nos. 61201064 and 51332003).

References

1. D. Lin, Q. Zheng, Y. Li, Y. Wan, Q. Li, W. Zhou, Microstructure, ferroelectric and piezoelectric properties of $Bi_{0.5}K_{0.5}TiO_3$-modified $BiFeO_3$–$BaTiO_3$ lead-free ceramics with high Curie temperature. J. Eur. Ceram. Soc. **33**, 3023–3036 (2013)
2. L. Shi, B. Zhang, Q. Liao, L. Zhu, L. Zhao, D. Zhang, D. Guo, Piezoelectric properties of Fe_2O_3 doped $BiYbO_3$–Pb(Zr, Ti)O_3 high Curie temperature ceramics. Ceram. Int. **40**, 11485–11491 (2014)
3. Y. Saito, H. Takao, T. Tani, T. Nonoyama, K. Takatori, T. Homma, T. Nagaya, M. Nakamura, Lead-free piezoceramics. Nature **432**, 84–87 (2004)
4. S.K. Patri, R.N.P. Choudhary, Solid solutions of bismuth-based Aurivillius oxides: structural and dielectric characterization. Appl. Phys. A **94**, 321–327 (2009)
5. X. Zheng, X. Huang, C. Gao, Study on ferroelectric and dielectric properties of La-doped $CaBi_4Ti_4O_{15}$ based ceramics. J. Rare Earths **25**, 168–172 (2007)
6. H. Hao, H.X. Liu, M.H. Cao, X.M. Min, S.X. Ouyang, Study of A-site doping of $SrBi_4Ti_4O_{15}$ Bi-layered compounds using micro-Raman spectroscopy. Appl. Phys. A **85**, 69–73 (2006)
7. P.K. Panda, Review: environmental friendly lead-free piezoelectric materials. J. Mater. Sci. **44**, 5049–5062 (2009)
8. Z.G. Yi, Y.X. Li, Y. Liu, Ferroelectric and piezoelectric properties of Aurivillius phase intergrowth ferroelectrics and the underlying materials design. Phys. Status Solidi A **208**, 1035–1040 (2011)
9. X. Huang, Z. Chen, X. Zheng, C. Gao, H. Guan, C. Zhao, Dielectric and piezoelectric properties of $Ca_{1-x}(Li, Ce)_{x/2}Bi_4Ti_4O_{15}$ ceramics. J. Rare Earths **25**, 158–162 (2007)
10. C.M. Wang, J.F. Wang, J.A. Ceram, Aurivillius phase potassium bismuth titanate: $K_{0.5}Bi_{4.5}Ti_4O_{15}$. J. Am. Ceram. Soc. **91**, 918–923 (2008)
11. S. Kumar, S. Kundu, D.A. Ochoa, J.E. Garcia, K.B.R. Varma, Raman scattering, microstructural and dielectric studies on $Ba_{1-x}Ca_xBi_4Ti_4O_{15}$ ceramics. Mater. Chem. Phys. **136**, 680–687 (2012)
12. J.R. Gomah-Pettry, E. Said, P. Marchet, M. Jean-Pierre, Sodium-bismuth titanate based lead-free ferroelectric materials. J. Eur. Ceram. Soc. **24**, 1165–1169 (2004)
13. Z.G. Gai, Y.Y. Feng, J.F. Wang, M.L. Zhao, L.M. Zheng, C.M. Wang, S.J. Zhang, T.R. Shrout, The effect of (Li, Ce) doping in Aurivillius phase material $(Na_{0.52}K_{0.42}Li_{0.06})_{0.5}Bi_{2.5}(Nb_{1.88}Sb_{0.06}Ta_{0.06})O_9$. Phys. Status Solidi A **207**, 1792–1795 (2010)
14. H.T. Zhang, H.X. Yan, M.J. Reece, The effect of Nd substitution on the electrical properties of Bi_3NbTiO_9 Aurivillius phase ceramics. J. Appl. Phys. **106**, 044106 (2009)
15. W. Wang, D. Shan, J.B. Sun, X.Y. Mao, X.B. Chen, Aliovalent B-site modification on three- and four-layer. Aurivillius intergrowth. J. Appl. Phys. **103**, 044102 (2008)
16. Z. Peng, Q. Chen, D. Liu, Y. Wang, D. Xiao, J. Zhu, Evolution of microstructure and dielectric properties of (LiCe)-doped $Na_{0.5}Bi_{2.5}Nb_2O_9$ Aurivillius type ceramics. Curr. Appl. Phys. **13**, 1183–1187 (2013)
17. H. Chen, B. Shen, X. Jinbao, J. Zhai, Textured $Ca_{0.85}(Li, Ce)_{0.15}Bi_4Ti_4O_{15}$ ceramics for high temperature piezoelectric applications. Mater. Res. Bull. **47**, 2530–2534 (2012)

18. C.L. Diao, H.W. Zheng, Y.Z. Gu, W.F. Zhang, L. Fang, Structural and electrical properties of four-layers Aurivillius phase $BaBi_{3.5}Nd_{0.5}Ti_4O_{15}$ ceramics. Ceram. Int. **40**, 5765–5769 (2014)
19. P. Fang, P. Liu, Z. Xi, W. Long, X. Li, Structure and electrical properties of new Aurivillius oxides $(K_{0.16}Na_{0.84})_{0.5}Bi_{4.5}Ti_4O_{15}$ with manganese modification. J. Alloys Compd. **595**, 148–152 (2014)
20. A. Tanwar, M. Verma, V. Gupta, K. Sreenivas, A-site substitution effect of strontium on bismuth layered $CaBi_4Ti_4O_{15}$ ceramics on electrical and piezoelectric properties. Mater. Chem. Phys. **130**, 95–103 (2011)
21. H.X. Yan, Z. Zhang, W.M. Zhu, The effect of (Li, Ce) and (K, Ce) doping in Aurivillius phase material $CaBi_4Ti_4O_{15}$. Mater. Res. Bull. **39**, 1237–1246 (2004)
22. J. Zeng, Y. Li, D. Wang, Q. Yin, Electrical properties of neodymium doped $CaBi_4Ti_4O_{15}$ ceramics. Solid State Comm. **133**, 553–557 (2005)
23. Y.Y. Yao, C.H. Song, P. Bao, D. Su, X.M. Lu, J.S. Zhu, Y.N. Wang, Doping effect on the dielectric property in bismuth titanate. J. Appl. Phys. **95**, 3126 (2004)
24. Z. Zhou, X. Dong, H. Chen, Structural and electrical properties of W^{6+}-doped Bi_3TiNbO_9 high-temperature piezoceramics. J. Am. Ceram. Soc. **89**, 1756 (2006)
25. J.T. Zeng, Y. Wang, Y.X. Li, Q.B. Yang, Q.R. Yin, Ferroelectric and piezoelectric properties of tungsten doped $CaBi_4Ti_4O_{15}$ ceramics. J. Electroceram. **21**, 305–308 (2008)
26. S.J. Zhang, N. Kim, T.R. Shrout, High temperature properties of manganese modified $CaBi_4Ti_4O_{15}$ ferroelectric ceramics. Solid State Commun. **140**, 154–158 (2006)
27. D.G. Gu, G.R. Li, L.Y. Zheng, Electrical properties of Mn modified $CaBi_4Ti_4O_{15}$ piezoelectrics for high temperature application. J. Inorg. Mater. **23**, 626–630 (2008)
28. P. Fang, P. Liu, Z. Xi, W. Long, X. Li, Effect of cerium additives on structure and electrical properties of Aurivillius oxides $(K_{0.16}Na_{0.84})_{0.5}Bi_{4.5}Ti_4O_{15}$. Mater. Sci. Eng., B **186**, 21–25 (2014)
29. L.B. McCusker, R.B. Von Dreele, D.E. Cox et al., Rietveld refinement guidelines. J Appl Cryst. **32**, 36–50 (1999)
30. S.L. Chauhan, M. Kumar, S. Chhoker et al., Multiferroic, magnetoelectric and optical properties of Mn doped $BiFeO_3$ nanoparticles. Solid State Commun. **152**, 525–529 (2012)
31. Z.H. Peng, Q. Chen, J.G. Wu, Dielectric properties and impedance analysis in Aurivillius-type $(Na_{0.25}K_{0.25}Bi_{0.5})_{1-x}(LiCe)_{x/2}[]_{x/2}Bi_4Ti_4O_{15}$ ceramics. J Alloys Compd **541**, 310–316 (2012)
32. D.Y. Suarez, I.M. Reaney, W.E. Lee, Relation between tolerance factor and T_C in Aurivillius compounds. J. Mater. Res. **16**, 3139–3149 (2001)
33. W. Cai, F. Chunlin, Z. Lin, X. Deng, Vanadium doping effects on microstructure and dielectric properties of barium titanate ceramics. Ceram. Int. **37**, 3643–3650 (2011)
34. S.K. Rout, A. Hussain, E. Sinha, C.W. Ahn, I.W. Kim, Electrical anisotropy in the hot-forged $CaBi_4Ti_4O_{15}$ ceramics. Solid State Sci. **11**, 1144–1149 (2009)
35. H.X. Yan, C.G. Li, J.G. Zhou, W.M. Zhu, L.X. He, Y.X. Song, Y.H. Yu, Influence of sintering temperature on the properties of high T-c bismuth layer structure ceramics. Mater. Sci. Eng., B **88**, 62–67 (2002)
36. X. He, B. Wang, F. Xiaoyi, Z. Chen, Structural, electrical and piezoelectric properties of V-, Nb- and W-substituted $CaBi_4Ti_4O_{15}$ ceramics. J. Mater. Sci.: Mater. Electron. **25**, 3396–3402 (2014)
37. I. Coondoo, A.K. Jha, Enhancement of ferroelectric and piezoelectric characteristics in europium substituted $SrBi_2Ta_2O_9$ ferroelectric ceramics. Mater. Lett. **63**, 48–50 (2009)
38. X. Zhang, H. Yan, M.J. Reece, Effect of a site substitution on the properties of $CaBi_2Nb_2O_9$ ferroelectric ceramics. J. Am. Ceram. Soc. **91**, 2928–2932 (2008)
39. X.X. Tian, S.B. Qu, H.L. Du et al., Effects of (Li Ce) co-substitution on the structural and electrical properties of $CaBi_2Nb_2O_9$ ceramics. Chin. Phys. B **21**, 037701 (2012)
40. E.C. Subbarao, Family of ferroelectric bismuth compounds. J. Phys. Chem. Solids **23**, 665–676 (1962)